

# EXPERIMENT OF SOFT X-RAY GENERATIONS USING INVERSE COMPTON SCATTERING AT WASEDA UNIVERSITY

S. Kashiwagi, Y. Hama, H. Ishikawa, H. Kawai, R. Kuroda, K. Maeda, H. Nagasawa, T. Oshima,  
M. Washio, A. Yada, Waseda University, Tokyo, Japan  
H. Hayano, J. Urakawa, KEK, Ibaraki, Japan

## Abstract

One of the most promising approaches to short pulsed X-ray sources is the Laser Synchrotron Source (LSS). It is based on inverse Compton scattering between a pico-second electron beam and a pulsed laser light. On the other hand, soft X-ray source is very powerful tool for biological observation. The soft X-ray source using inverse Compton scattering between 5 MeV electron beam produced by a photo-cathode rf-gun and an IR pulsed laser light (1047 nm) obtained from an all-solid state Nd:YLF laser is developing at Waseda University. In future, this soft X-ray source will be applied to a X-ray microscopy to observe hydrated biological specimens. In this conference, the experiment of soft X-ray generation at Waseda University will be described.

## 1 INTRODUCTION

Short-pulsed X-ray source is required in various research fields, such as material and medical science. To meet these demands, R&D on the next-generation light source has been initiated at several laboratories in the world. One of the most promising approaches to short-pulsed X-ray sources is the Laser Synchrotron Source (LSS), which is based on inverse Compton scattering. Inverse Compton scattering between a relativistic electron beam and a laser light has been investigated as a technique of high bright X-ray generation [1-3]. The LSS has many features, which are tunability of the wavelength, the spectrum distribution, the spatial distribution and the yield of the scattered photons. Those characteristics of scattered photons can be controlled varying the collision angle between the electron beam and the laser pulse, changing energy of the electron beam or wavelength of the laser light. Further, ultra-short pulsed X-ray generations were developed based on scattering between a short-bunched electron beam and a femto-second high power laser pulse in 90 degrees interaction [4].

Experiment of soft X-ray generation via inverse Compton scattering is performed at Waseda University. Soft X-rays are very useful for biological observation, because K-shell absorption edges of Oxygen, Carbon and Nitrogen, which mainly constitute of a living body, are 2.322 nm, 4.368nm and 3.099 nm, respectively [5] and those absorption edges are included in the range of “water window”. Since the absorption coefficient of water is much smaller than the protein’s coefficient in this range of “water window”, a dehydration of the specimens is not necessary. In future, the soft X-ray source will be applied to an X-ray microscopy to get the images of hydrated

biological specimens without blurring caused by radiation damage and thermal diffusion.

## 2 X-RAY GENERATION

In the inverse Compton scattering, the wavelength of generated soft X-rays can be changed by the collision angle between the electron beam and the laser lights. It is assumed that electron beam energy and incident photon energy are  $E_b (= \gamma mc^2)$  and  $k_0$  in the laboratory frame. The energy of scattered photons  $k_s$  is given as

$$k_s = \frac{\gamma^2 k_0 (mc^2)(1 + \beta \cos \varphi)(1 + \beta \cos \theta)}{mc^2 + (1 + \cos \theta)(1 + \beta \cos \varphi)\gamma k_0}, \quad (1)$$

where  $\cos \theta = (\cos \theta_s - \beta)/(1 - \beta \cos \theta_s)$ , angles of  $\varphi$ ,  $\theta$ ,  $\theta_s$  are the crossing angle in the laboratory frame, the scattered angle in the electron rest frame and the laboratory frame, respectively. From Equation (1), the maximum energy of scattered photons is given as

$$k_s(\max) = \frac{\gamma^2 k_0 (mc^2)(1 + \beta \cos \varphi)(1 + \beta)}{mc^2 + 2 \cdot (1 + \beta \cos \varphi)\gamma k_0} \quad (2)$$

Figure 1 gives the scattered angles versus the scattered photon energy with different collision angles and the energy of K-shell absorption edge of Oxygen, Carbon and Nitrogen. In the Figure 1, it is assumed that the energy of electron beam is 5 MeV and the wavelength of laser is 1047 nm. To select the energy of the generated X-rays, they will be collected within a few degrees along the direction of the electron beam propagation.

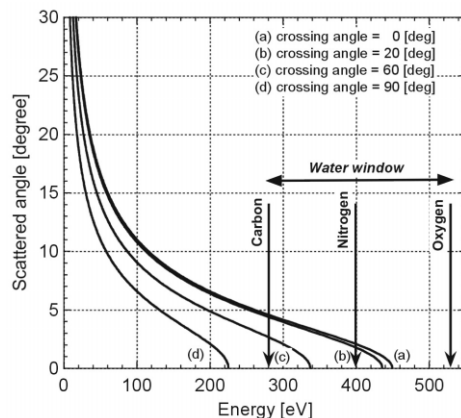


Figure 1: Angular distribution of scattered X-rays at different crossing angle. K-shell absorption edge of Carbon, Nitrogen and Oxygen.

The total number of produced X-ray photons by inverse Compton scattering is given by the product of the cross section of Compton scattering ( $\sigma$ ) and Luminosity ( $L$ ), which is determined by the scattering geometry of the electron beam and the laser pulse. In the case of head-on configuration (zero crossing angle), the number of generated X-ray photons is generally maximized. Figure 2 shows the differential cross section, which was derived from Klein-Nishina Formula, as the function of the generated X-ray energy at difference crossing angles.

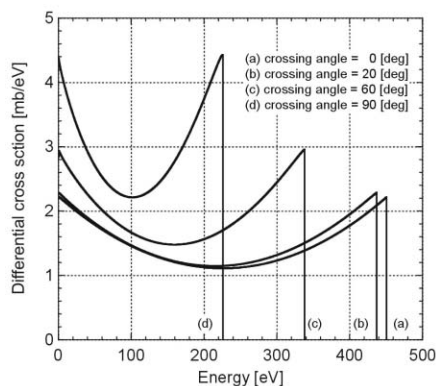


Figure 2: Differential cross section as the function of the generated X-ray energy in different crossing angles.

### 3 X-RAY GENERATION EXPERIMENT AT WASEDA UNIVERSITY

#### 3.1 Experimental setup

Beam line layout for X-ray generation experiment is shown in Figure 3. In our X-ray generation experiment, a stable laser light (1047 nm) is scattered by the pulsed electron beam, which is produced by a photo-cathode rf-gun system. The rf-gun system is composed of the BNL type 1.6 cells S-band rf cavities with Mg cathode [6,7] and a stabilized all-solid-state laser and an rf power source. All-solid-state pico-second Nd:YLF laser is used for both an irradiation of the rf-gun cathode and the inverse Compton scattering. The electron beam is emitted from the Mg photo-cathode using the 10 ps UV laser light (262 nm). The electron beam can be controlled very precisely changing the injection phase, the intensity and the profiles in transverse and longitudinal directions of the laser pulses. The produced electron beam is focused at center of an interaction chamber using a solenoid magnet and the quadrupole magnets. The timing jitter between the electron bunch and Nd:YLF laser light for inverse Compton scattering is negligible in comparison with the pulse length of the electron beam and the laser light, since the seed of UV laser pulse for the photo-cathode illumination of the rf-gun and IR laser pulse is same seed laser light (Figure 4).

The interaction chamber for the inverse Compton scattering experiment was designed to select the crossing angle, 20, 60 and 90 degrees, between the electron beam and the laser light. Choosing the crossing angles, the energy spectrum of the generated X-rays can be changed

with constant operation of accelerator and laser system. Furthermore, the energy of generated X-rays with pulse-to-pulse can be changed by controlling the laser injection angle to the interaction chamber with combination of Pockels cells and polarizers.

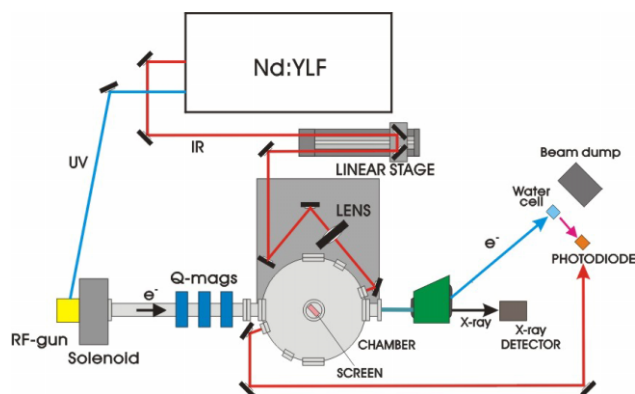


Figure 3: Beam line layout for X-ray generation experiment.

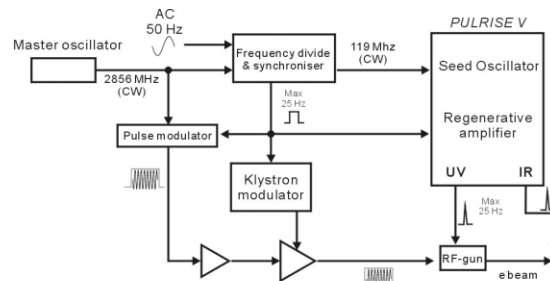


Figure 4: Rf and timing diagram for the rf-gun and the laser system

About 2 mJ, 10 ps (FWHM) pulsed Nd:YLF (IR: 1047nm) laser beam is introduced through the window and focused at the center of the interaction chamber. After interaction, laser beam go through from the opposite window. A dipole magnet separates the electron beam and the scattered soft X-rays after the interaction point (shown in Figure 3). Soft X-rays are measured using a circular microchannel plate (MCP), which is located 0.6 m from interaction point of the electron beam axis. The diameter of MCP sensitive area is 14.5 mm correspond to a collection angle  $\theta_s = 11$  mrad.

#### 3.2 Beam Experiment

Up to now, the electron beam and the laser pulse focusing have been tried at the interaction point. The 4 MeV electron bunch with 10 ps (FWHM), 1 nC were produced by the photo-cathode rf-gun and tried to focused into small beam-spot at the interaction point to get high luminosity. However, we couldn't be achieved the good focusing of electron beam. It should be limited due to space charge effect and chromatic effect from energy spread. The focused horizontal and vertical electron beam sizes were about 300  $\mu\text{m}$ . IR laser pulses were focused into about  $\sigma_L = 80$   $\mu\text{m}$  using a optical lens, which is 300 mm focal length.

Timing adjustment between electron beam and laser pulse has been performed using a remote optical delay line whose active-length is 20 cm (correspond to 1.3 ns optical delay). To adjust a timing of the scattering, the signals of electron beam and laser pulse have been monitored using a fast photodiode detector, the electron beam signal was Cherenkov radiation, which was generated when the electron beam pass through a water cell at the end of 45 degree beam line (shown in Figure 3). Figure 5 shows typical observed photodiode signal of electron beam and laser pulse.

Spatial alignment between electron beam and laser pulse have been done using a screen monitor that is consist of a 100  $\mu\text{m}$  thickness phosphor screen and a 300  $\mu\text{m}$  thickness aluminium plate with a 600  $\mu\text{m}$  diameter hole. Both of the focused electron beam and laser pulse were align to the small hole of the screen monitor.

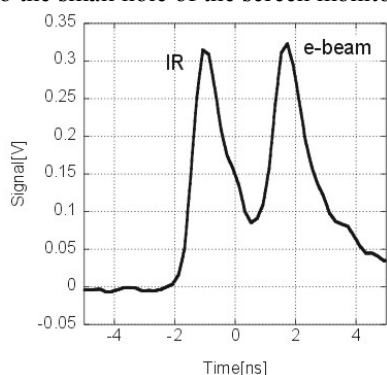


Figure 5: Typical scope-trace of photodiode output shows the electron beam signal (Cherenkov light) and IR laser light.

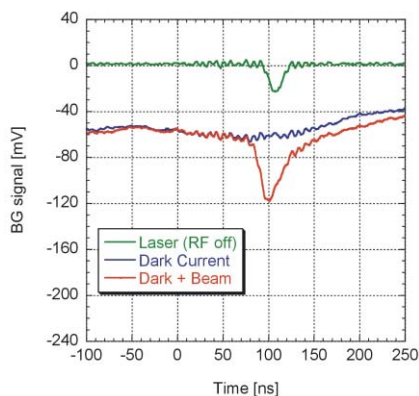


Figure 6: Background signal of X-ray detector

Background observation has been done. Figure 6 shows the measured background signals under the different conditions. Main background sources were beamsstrahlung of the electron beam and a dark current from rf-gun cavities due to a field emission. They have different time structure, the pulse width of dark current so much longer than beamsstrahlung, therefore we can distinguish these two background noises. We have known that a scattered UV laser light on the cathode surface also make a noise for the X-ray detection, it is shown in Figure 6 as a green line (upper line).

### 3.3 Result and discussion

Until now, the pulsed X-ray signal wasn't observed using MCP detector. It requires that a precise spatial alignment between electron beam and laser light at the interaction point and a high luminosity of inverse Compton scattering, which will be achieved by good focusing of the electron beam and energy upgrade of IR laser pulse. In next operation for the X-ray generation experiment, electron beam will be focused into flat shape to relax the space charge effect without luminosity drop. Table 1 shows total number of generated X-ray photons with different horizontal and vertical beam size ratio.

$\sigma_h \backslash \sigma_v$	100	200	300
100	$1.8 \times 10^4$	$1.6 \times 10^4$	$1.3 \times 10^4$
200	$9.8 \times 10^3$	$8.7 \times 10^3$	$7.5 \times 10^3$
300	$6.7 \times 10^3$	$5.9 \times 10^3$	$5.2 \times 10^3$

Table 1: Total number of generated X-ray photons with 2nC electron beam and 2mJ IR laser pulse. Focal spot size of laser pulse is 60  $\mu\text{m}$ .

## 4 SUMMARY

Soft X-ray generation experiment using inverse Compton scattering has been started at Waseda University. The interaction chamber has been installed to the beam line and it is possible to make three different angle collisions between the electron beam and the IR laser pulse. To get high intense X-rays, a pulse amplifier for IR laser light will be install laser system and flat shape focusing of electron beam will be tried in next beam operation for X-ray generation experiment.

## 5 ACKNOWLEDGRMENT

Authors would like to express sincere thanks to Professor I. Ben-Zvi and Dr. X. J. Wang of BNL for their deep help on the development of the rf-gun and their insightful discussion. We would like to great thank Drs. A. Endo, M. Yorozu and Y. Aoki of SHI and FESTA group for their expert technical support about laser system. This research is supported in part by the Grant for special project of Waseda University, No. 2001B-043.

## 6 REFERENCES

- [1] W. Leemans et al., Proceeding of the 1995 Particle Accelerator Conference, 1995, p.174
- [2] S. Kashiwagi et al., Nuclear Instrument and Methods A 455, p. 36-40 (2000).
- [3] I. V. Pogorelsky, et al. , Phys. Rev. ST-AB, Vol.3: 090702, (1999)
- [4] M. Yorozu et al., Jpn. J. Appl. Phys. Vol. 40 (2001) pp.4228-4232 Part 1, N0.6A, June 2001
- [5] B. L. Henke et al., Atomic Data and Nuclear Data Tables 27, (1982).
- [6] T. Srinivasan-Rao et al., J. Appl. Phys. 77 (3) 77 (3), p. 1275-1279 (1995).
- [7] D. T. Palmer et al Proceeding of the 1997 Particle Accelerator Conference, 1997, p. 2843.